

Analytical structure of the equation of state at finite density: Resummation versus expansion in a low energy model

Swagato Mukherjee,¹ Fabian Rennecke,^{1,2,3,*} and Vladimir V. Skokov^{4,5}

¹*Department of Physics, Brookhaven National Laboratory, Upton, New York 11973, USA*

²*Institute for Theoretical Physics, Justus Liebig University Giessen,
Heinrich-Buff-Ring 16, 35392 Giessen, Germany*

³*Helmholtz Research Academy Hesse for FAIR (HFHF), Campus Giessen, 35392 Giessen, Germany*

⁴*Department of Physics, North Carolina State University, Raleigh, NC 27695, USA*

⁵*RIKEN BNL Research Center, Brookhaven National Laboratory, Upton, New York 11973, USA*

(Dated: March 30, 2022)

For theories plagued with a sign problem at finite density, a Taylor expansion in the chemical potential is frequently used for lattice gauge theory based computations of the equation of state. Recently, in arXiv:2106.03165, a new resummation scheme was proposed for such an expansion that resums contributions of correlation functions of conserved currents to all orders in the chemical potential. Here, we study the efficacy of this resummation scheme using a low energy model, namely the mean-field quark-meson model. After adapting the scheme for a mean-field analysis, we confront the results of this scheme with the direct solution of the model at finite density as well as compare with results from Taylor expansions. We study to what extent the two methods capture the analytical properties of the equation of state in the complex chemical potential plane. As expected, the Taylor expansion breaks down as soon as the baryon chemical potential reaches the radius of convergence defined by the Yang-Lee edge singularity. Encouragingly, the resummation not only captures the location of the Yang-Lee edge singularity accurately, but is also able to describe the equation of state for larger chemical potentials beyond the location of the edge singularity for a wide range of temperatures.

I. INTRODUCTION

Uncovering the structure of the phase diagram of Quantum Chromodynamics at nonzero temperature and density has been the central goal for both the theoretical and the experimental nuclear physics community (see Ref. [1] for a review). Non-perturbative theoretical understanding of the QCD phase diagram is hampered by the so-called sign problem. To introduce it, we consider a theory containing bosonic fields Φ and fermionic fields ψ in Euclidean spacetime with the following classical action

$$S[\Phi, \psi, \bar{\psi}] = S_{\Phi}[\Phi] + \int_0^{\beta} dx_0 \int d^3x \bar{\psi}(x) M(\Phi; \mu) \psi(x). \quad (1)$$

Here S_{Φ} is the part of the action that only depends on Φ . $M(\Phi; \mu)$ is a Dirac operator which includes a coupling between the fermionic and bosonic fields. We are considering finite temperature $T = 1/\beta$ and finite chemical potential μ . Thus the Dirac operator, as indicated above, explicitly depends on the chemical potential μ . A prominent example of such a theory is QCD with the bosonic fields to be identified with gluons and the fermionic fields with quarks.

The partition function of this theory can formally be obtained from the Euclidean path integral,

$$Z = \int \mathcal{D}\Phi \mathcal{D}\psi \mathcal{D}\bar{\psi} e^{-S}. \quad (2)$$

The grand canonical thermodynamic potential Ω is then proportional to $\ln Z$. The action in Eq. (1) is quadratic in the fermionic fields; therefore they can be readily integrated out, resulting in the (non-local) functional fermionic determinant $\det M$,

$$Z = \int \mathcal{D}\Phi \exp \left[-S_{\Phi}[\Phi] + \ln \det M(\Phi; \mu) \right]. \quad (3)$$

In numerous theories, including QCD, the presence of a finite chemical potential in the Dirac operator gives rise to a sign problem: a real μ can lead to a complex spectrum of the Dirac operator. In this case the weight of the configurations of Φ , $\sim \det M$, is complex, rendering the Monte-Carlo importance sampling impractical.

Aside from attempts to entirely circumvent the sign problem, e.g. by using methods that do not have to rely on importance sampling [2–10], a common strategy is to expand the path integral about $\mu = 0$ [11, 12]. This yields a power series in μ , where each coefficient can be computed from the path integral with the $\mu = 0$ weight. Information at finite μ is therefore obtained through an extrapolation from $\mu = 0$.

Although improvements of the the conventional Taylor expansion have been proposed in the literature [13], a major obstacle for schemes based on analytical expansions is that they are bound by the analytical constraints of the underlying theory. Singularities in the complex plane determine the radius of convergence of analytical expansions. Resummations based on Padé approximations can be used to estimate the location of the (nearest) singularities, see, e.g., [12, 14–17]. Still, precise knowledge of expansion coefficients of very high order is required and information

* fabian.rennecke@theo.physik.uni-giessen.de

beyond the singularities are difficult to obtain.

In this work, we study the approach introduced in [18], where contributions of ($n \leq N$)-point correlation functions of the fermion number currents to the thermodynamic potential are resummed to all orders in μ . In addition to improved convergence, zeros of the partition function of QCD at imaginary μ have been identified, which could be related to physical singularities of the thermodynamic potential. The main motivation of this work is to examine this in detail regarding the analytic and thermodynamic properties of a model where these quantities can be computed directly.

To this end, we use a quark-meson model which can be solved directly in mean-field approximation. While simplistic, this model captures some basic features of QCD at low energies and of the chiral phase transition, see, e.g., [19–23] for studies in mean-field and beyond. After introducing the resummation scheme and adapting it to a mean-field approximation in Sec. II, we introduce the model in Sec. III. In Sec. IV we discuss the analytical properties of the model for complex chemical potential and study how well it can be reproduced by the resummation scheme. Full results for the thermodynamics at real and imaginary chemical potentials are confronted with the resummation and the conventional Taylor expansion in Sec. V.

II. RESUMMATION

We start by introducing the resummation scheme of Ref. [18]. To this end, we define the derivatives of the logarithm of the fermion determinant as

$$D_n(\Phi) = \left. \frac{\partial^n \ln \det M(\Phi; \mu)}{\partial \hat{\mu}^n} \right|_{\mu=0}, \quad (4)$$

with $\hat{\mu} = \mu/T$. Expanding the fermion determinant inside the path integral to order N in powers of $\hat{\mu}$ yields

$$\begin{aligned} Z_N^R &= \int \mathcal{D}\Phi \exp \left[\sum_{n=1}^N \frac{1}{n!} D_n(\Phi) \hat{\mu}^n \right] \det M(\Phi; 0) e^{-S_\Phi[\Phi]} \\ &= \left\langle \exp \left[\sum_{n=1}^N \frac{1}{n!} D_n(\Phi) \hat{\mu}^n \right] \right\rangle_0. \end{aligned} \quad (5)$$

The ensemble average at $\mu = 0$ is given by

$$\langle A \rangle_0 = \int \mathcal{D}\Phi A \det M(\Phi; 0) e^{-S_\Phi[\Phi]}. \quad (6)$$

The resulting thermodynamic potential is

$$\Omega_N^R(T, \mu) = -\frac{T}{V} \ln Z_N^R, \quad (7)$$

where V is the spatial volume. Crucially, even at finite order of the expansion, N , Ω_N^R contains infinite powers of $\hat{\mu}$.

In contrast, an ordinary Taylor expansion of the thermodynamic potential about $\mu = 0$ to order N ,

$$\Omega_N^E(T, \mu) = \sum_{n=1}^N \frac{1}{n!} \left. \frac{\partial^n \Omega(T, \mu)}{\partial \hat{\mu}^n} \right|_{\hat{\mu}=0} \hat{\mu}^n, \quad (8)$$

is only an N -th order polynomial of $\hat{\mu}$ by construction. In theories with charge conjugation symmetry (including QCD), only even powers of $\hat{\mu}$ contribute in Eq. (8). Ω_N^E can be expressed in terms of averages of the D_n at $\mu = 0$ [24]. As pointed out in [18], Ω_N^R can be interpreted as an all-order resummation of finite-order contributions to Ω_N^E . This resummation is directly connected to the reweighting method; for recent developments see, e.g., [25, 26]. Expanding the logarithm of the fermion determinant in the weight $\det M(\Phi; \mu)/\det M(\Phi; 0)$ in powers of μ leads to Eq. (5).

Naturally, the nontrivial analytic structure of the thermodynamic potential in plane of complex μ , see [27, 28], cannot be captured by a strictly analytic expansion in μ . Yet, the closest singularity in the complex plane determines the radius of convergence of the expansion. Both Ω_N^R and Ω_N^E can be evaluated at complex μ . However, unlike Ω_N^E , which cannot resolve such singularities (directly), $\text{Re}[Z_N^R]$ in Eq. (5) can become negative, resulting in a singular Ω_N^R .

In this work, we want to test Eq. (7) using a mean-field approximation, i.e. to leading order in the saddle point approximation of the path integral. In general, the thermodynamic potential on a background field $\bar{\Phi}$ is

$$\bar{\Omega}(T, \mu; \bar{\Phi}) = -\frac{T}{V} \left\{ S_\Phi[\bar{\Phi}] + \ln \det M(\bar{\Phi}; \mu) \right\}, \quad (9)$$

and the stationary point $\bar{\Phi}_0$ is determined by

$$\left. \frac{\delta \bar{\Omega}(T, \mu; \bar{\Phi})}{\delta \bar{\Phi}} \right|_{\bar{\Phi}_0} = 0. \quad (10)$$

Correspondingly, Eq. (7) becomes

$$\begin{aligned} \bar{\Omega}_N^R(T, \mu; \bar{\Phi}) &= -\frac{T}{V} \left\{ S_\Phi[\bar{\Phi}] + \ln \det M(\bar{\Phi}; 0) \right. \\ &\quad \left. + \sum_{n=1}^N \frac{1}{n!} D_n(\bar{\Phi}) \hat{\mu}^n \right\}. \end{aligned} \quad (11)$$

Since the expansion in $\hat{\mu}$ in Eq. (5) is done before the ensemble average, the stationary point $\bar{\Phi}_0^R$ is defined by Eq. (11),

$$\left. \frac{\delta \bar{\Omega}_N^R(T, \mu; \bar{\Phi})}{\delta \bar{\Phi}} \right|_{\bar{\Phi}_0^R} = 0, \quad (12)$$

and all thermodynamic quantities can be extracted from

$$\bar{\Omega}_N^R(T, \mu) \equiv \bar{\Omega}_N^R(T, \mu; \bar{\Phi}_0^R). \quad (13)$$

Owing to the explicit μ -dependence of $\bar{\Omega}_N^R(T, \mu; \bar{\Phi})$, the stationary point of the resummed expansion depends

nontrivially on μ , $\bar{\Phi}_0^R = \bar{\Phi}_0^R(\mu)$. Through this dependence, $\bar{\Omega}_N^R$ is in general a nonanalytic function of μ .

This is in contrast to the ordinary Taylor expansion in mean-field,

$$\bar{\Omega}_N^E(T, \mu) = - \sum_{n=0}^N \frac{\chi_n(0)}{n!} \hat{\mu}^n, \quad (14)$$

where the coefficients are given by the the susceptibilities,

$$\chi_n(\mu) = \frac{T}{V} \frac{\partial^n \bar{\Omega}(T, \mu; \bar{\Phi}_0)}{\partial \hat{\mu}^n}, \quad (15)$$

evaluated at $\mu = 0$ and therefore do not depend on μ . For any finite N , $\bar{\Omega}_N^E$ is a finite (N -th) order polynomial in μ^2 and hence $\bar{\Omega}_N^E$ is strictly analytic.

III. MODEL

To test the resummation scheme of [18] directly, we use a quark-meson model with $N_f = 2$ degenerate quark flavors and $N_c = 3$ colors. The Euclidean action is

$$S^{\text{QM}} = \int_0^\beta dx_0 \int d^3x \left\{ \bar{\psi} \left(\gamma_\mu \partial_\mu + \frac{1}{2} h \boldsymbol{\tau} \boldsymbol{\phi} + \gamma_0 \mu \right) \psi + \frac{1}{2} (\partial_\mu \boldsymbol{\phi})^2 + U(\boldsymbol{\phi}^2) - j\sigma \right\}. \quad (16)$$

γ_μ are the Euclidean gamma matrices, $\boldsymbol{\tau}^T = (1, i\gamma_5 \vec{\tau})$ with the Pauli matrices $\vec{\tau}$, and $\boldsymbol{\phi}^T = (\sigma, \vec{\pi})$ is the $O(4)$ meson field. $U(\boldsymbol{\phi}^2)$ is the $O(4)$ symmetric effective meson potential. An explicit symmetry breaking is introduced through the source j , which can be related to the current quark mass. The precise form of this relation is of no importance for our study.

In this work we employ a mean-field approximation to compute the thermodynamic potential Ω based on Eq. (16). Assuming a homogeneous mean field, the meson background field is

$$\bar{\boldsymbol{\phi}} = \begin{pmatrix} \bar{\sigma} \\ \vec{0} \end{pmatrix}, \quad (17)$$

resulting in the Dirac operator

$$M^{\text{QM}}(\bar{\sigma}; \mu) = \gamma_\mu \partial_\mu + \gamma_0 \mu + \frac{1}{2} h \bar{\sigma}, \quad (18)$$

where the appropriate unit matrices in spinor-, color- and flavor space are implied. The thermodynamic potential then is

$$\bar{\Omega}^{\text{QM}}(T, \mu; \bar{\sigma}) = U(\bar{\boldsymbol{\phi}}^2) - j\bar{\sigma} - \frac{T}{V} \ln \det M^{\text{QM}}(\bar{\sigma}; \mu), \quad (19)$$

The quark determinant $\det M$ can be evaluated using conventional methods of thermal field theory, see, e.g., [29].

With the fermionic Matsubara frequency $\nu_n = (2n+1)\pi T$ and the quark energy $E_q(\bar{\sigma}) = \sqrt{q^2 + \frac{1}{4} h^2 \bar{\sigma}^2}$, where $q^2 \equiv \vec{q}^2$, it reads

$$\begin{aligned} & \frac{T}{V} \ln \det M^{\text{QM}}(\bar{\sigma}; \mu) \\ &= 2N_f N_c T \sum_{n=-\infty}^{\infty} \int_q \ln \left[(\nu_n + i\mu)^2 + E_q(\bar{\sigma})^2 \right] \\ &\equiv 2N_f N_c \left[J_0(\bar{\sigma}) + J_{T, \mu}(\bar{\sigma}) + J_{T, -\mu}(\bar{\sigma}) \right], \end{aligned} \quad (20)$$

where we used the shorthand notation $\int_q = \int \frac{d^3q}{(2\pi)^3}$. The thermal contribution to the quark determinant is given by

$$J_{T, \mu}(\bar{\sigma}) = \frac{1}{2\pi^2} \int_0^\infty dq q^2 T \ln \left[1 + e^{-(E_q(\bar{\sigma}) - \mu)/T} \right]. \quad (21)$$

Away from the low- and high-temperature limits, this integral has to be carried out numerically. The vacuum contribution J_0 is ultraviolet-divergent. Nonetheless, the finite piece of the vacuum contribution may and does depend on the meson field. This contribution has to be carefully extracted [21]. For this we perform the expansion around $d = 3 - 2\epsilon$ dimension. It yields

$$J_0(\bar{\sigma}) = - \frac{h^4 \bar{\sigma}^4}{2^9 \pi^2 \Lambda^{2\epsilon}} \left[\frac{1}{\epsilon} - \ln \left(\frac{h^2 \bar{\sigma}^2}{4\Lambda^2} \right) + C + \mathcal{O}(\epsilon) \right], \quad (22)$$

with the constant $C = \ln(4\pi) - \gamma_E + \frac{3}{2}$, where γ_E is the Euler Mascheroni constant. Λ is the renormalization scale parameter. We subtract the divergent piece and the constant, take the limit $\epsilon \rightarrow 0$, and arrive at the vacuum contribution in dimensional regularization,

$$J_0^\epsilon(\bar{\sigma}) = \frac{h^4 \bar{\sigma}^4}{2^9 \pi^2} \ln \left(\frac{h^2 \bar{\sigma}^2}{4\Lambda^2} \right). \quad (23)$$

For the symmetric meson potential we use an ansatz which allows for spontaneous symmetry breaking,

$$U(\boldsymbol{\phi}^2) = \frac{\lambda}{4} (\boldsymbol{\phi}^2 - \nu^2)^2, \quad (24)$$

so that the regularized thermodynamic potential in the mean-field approximation becomes

$$\begin{aligned} \bar{\Omega}^{\text{QM}}(T, \mu; \bar{\sigma}) &= \frac{\lambda}{4} (\bar{\sigma}^2 - \nu^2)^2 - j\bar{\sigma} \\ &\quad - 2N_f N_c \left[J_0^\epsilon(\bar{\sigma}) + J_{T, \mu}(\bar{\sigma}) + J_{T, -\mu}(\bar{\sigma}) \right]. \end{aligned} \quad (25)$$

The vacuum contribution of the quarks is given in Eq. (23) and the thermal contribution in Eq. (21). Physical results are extracted the minimum of the thermodynamic potential, that is

$$\bar{\Omega}^{\text{QM}}(T, \mu) = \bar{\Omega}^{\text{QM}}(T, \mu; \bar{\sigma}_0), \quad (26)$$

h	$2 \times 300/93$
λ	21
ν	106 MeV
j	$138^2 \times 93 \text{ MeV}^3$
Λ	500 MeV
f_π	92.67 MeV
m_π	138.25 MeV
m_σ	496.59 MeV
T_{pc}	163.62 MeV
$(T_{CEP}, \mu_{B,CEP})$	(27.46, 895.85) MeV

TABLE I. Model parameters (upper half) and resulting physical quantities (lower half). T_{pc} is the pseudocritical temperature at $\mu_B = 0$, defined via the maximum of the correlation length m_σ^{-1} . $(T_{CEP}, \mu_{B,CEP})$ is the location of the critical endpoint. $\mu_B = 3\mu$ is the baryon chemical potential.

where $\bar{\sigma}_0$ is the solution of the equation of motion,

$$\left. \frac{\partial \bar{\Omega}^{QM}(T, \mu; \bar{\sigma})}{\partial \bar{\sigma}} \right|_{\bar{\sigma}_0} = 0. \quad (27)$$

The influence of the vacuum contribution on the thermodynamics of the quark-meson model has been studied in [21].

We thus have all ingredients of the model fully determined, as Eqs. (25) and (27) can numerically be solved for an arbitrary (complex) μ . Using Eqs. (11) and (12) we compute the resummed thermodynamic potential $\bar{\Omega}_N^{QM,R}$. The corresponding expansion coefficients D_n in Eqs. (11) are given by

$$D_n^{QM}(\bar{\sigma}) = \frac{2N_f N_c V}{T} \frac{\partial^n}{\partial \hat{\mu}^n} [J_{T,\mu}(\bar{\sigma}) + J_{T,-\mu}(\bar{\sigma})] \Big|_{\mu=0}, \quad (28)$$

where $J_{T,\mu}$ is defined in Eq. (21). Furthermore, using Eqs. (14) and (15) we compute the expanded and truncated thermodynamic potential $\bar{\Omega}_N^{QM,E}$. This is done by first computing $\bar{\Omega}^{QM}(T, \mu)$ in Eq. (26) for a small region of chemical potentials around $\mu = 0$ and then taking numerical derivatives at $\mu = 0$ to get the susceptibilities $\chi_n^{QM}(0)$ defined in Eq. (15). Table I shows the model parameters and resulting physical quantities we use for the numerical analysis. We use the baryon chemical potential $\mu_B = 3\mu$ in the following.

IV. ANALYTIC STRUCTURE

We first study how well the different methods capture the analytical structure of the model in the complex μ_B -plane. Phase transitions in the system are related to a branch cut in the thermodynamic potential at complex μ_B . At a second (first) order phase transition this cut

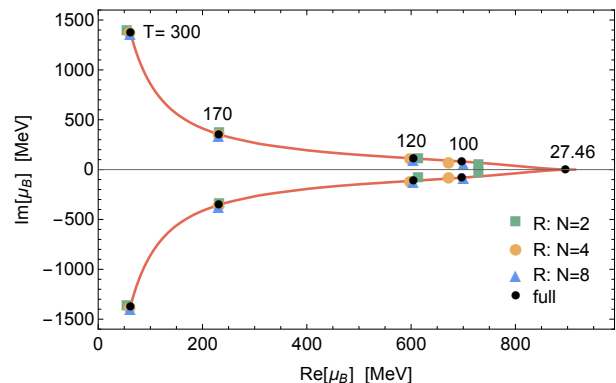


FIG. 1. Location of the Yang-Lee edge singularities in the complex right half plane of μ_B for $T = 1 - 300$ MeV. The red line shows the location of the full result. The points illustrate the location for specific temperatures, where the full result is compared to the resummed result at different truncation orders. For $T \lesssim 90$ MeV, the resummation method does not provide reliable results on the location of the edge singularity. For $T < T_{CEP} = 27.46$ MeV, instead of the edge singularity, there is a cut across the real axis, reflecting a first order phase transition.

pinches (crosses) the real μ_B axis. In the symmetric phase above the phase transition, the cut terminates at complex conjugate branch points, known as the Yang-Lee edge singularity μ_B^{YL} [27, 28]. In the vicinity of the pseudocritical temperature the closest singularity to the origin $\mu_B = 0$ is related to the second order phase transition in the chiral limit. Indeed, it has been shown by Fisher [30] that, at a given temperature, the Yang-Lee edge singularity corresponds to a critical point in the complex plane. For a more detailed discussion on this topic we refer to [31], see also [32–34]. To find the edge singularity μ_B^{YL} , we can follow the same procedure as when finding a critical point, that is we solve the system of equations

$$\begin{aligned} \frac{\partial \bar{\Omega}^{QM}(T, \mu_B/3; \bar{\sigma})}{\partial \bar{\sigma}} &= 0, \\ \frac{\partial^2 \bar{\Omega}^{QM}(T, \mu_B/3; \bar{\sigma})}{\partial \bar{\sigma}^2} &= 0. \end{aligned} \quad (29)$$

In contrast to a conventional critical point, where we look at real parameters T and μ_B , here, for a given T we solve for real and imaginary parts of μ_B^{YL} and $\bar{\sigma}^{YL}$. Note that the system consists of four equations, as for complex μ_B , the thermodynamic potential is complex-valued. The results for the location of the edge singularity for temperatures between 1 and 300 MeV are shown in Fig. 1.

The truncated Taylor expansion is analytic for any N and thus cannot provide direct information about the location of the Yang-Lee edge (except through the analysis of the radius of the convergence of the expansion). In other words, for any given order N , there are no solutions of Eq. (29) with $\bar{\Omega}^{QM} \rightarrow \bar{\Omega}_N^{QM,E}$. In contrast to this, we find that the resummed thermodynamic potential can

provide direct information about the location of the Yang-Lee edge singularity. In order to test this, we also solve Eq. (29) using $\Omega_N^{\text{QM,R}}$. Even at order $N = 2$, the exact location is reproduced rather accurately. For a comparison of the result for different orders N and the exact location at different temperatures, see Fig. 1. In general, even the lowest order resummation gives precise results on the location of the edge singularity for $T \gtrsim 120$ MeV, and higher orders increase the precision of the result. The resummation converges a bit slower at lower temperatures, but accurate results can be achieved, e.g., for order $N = 8$ at $T = 100$ MeV. However, the resummation completely fails to describe the location of the edge singularity below $T \lesssim 90$ MeV. This is directly related to the absence of thermal cuts in the resummation scheme.

In addition to the singularity and cut associated to the Yang-Lee edge, there are also thermal cuts. These cuts basically follow from the analytical structure of Eq. (21) and are present even in a gas of free fermions. This can be seen from a small mass/ T expansion, which is valid in the symmetric phase,

$$J_{T,\mu_B}(\sigma) = -\frac{1}{\pi}T^4 \text{Li}_4(-e^{\frac{\mu_B}{3T}}) + \frac{1}{16\pi}h^2\sigma^2T^2 \text{Li}_2(-e^{\frac{\mu_B}{3T}}) + \mathcal{O}(\sigma^4). \quad (30)$$

The polylogarithm $\text{Li}_s(z)$ has a branch cut at $\text{Re } z > 1$ and $\text{Im } z = 0$. This translates into cuts in the complex μ_B plane at $\text{Re } \mu_B > 0$ and $\text{Im } \mu_B = 3(2n+1)\pi T$ with $n \in \mathbb{Z}$. In both the Taylor expansion and the resummation this term is expanded in powers of μ_B , so that these cuts cannot be resolved either way. We therefore limit our analysis to $|\mu_B| < 3\pi T$, as it cannot be valid beyond this point. This also implies that the periodicity of $6\pi T$ at purely imaginary μ_B of the quark-meson model cannot be captured by both schemes. In general, this follows from the fact that the power series expansion of $\text{Li}_s(-e^w)$ about $w = 0$ is only valid for $|w| < \pi$ [35].

In our analysis $|\mu_B^{\text{YL}}| > 3\pi T$ for $T \lesssim 80$ MeV. Thus, the thermal cut, rather than the the edge singularity, is the closest singularity at small temperatures. This explains why the determination of the edge singularity with the resummation scheme converges more slowly at smaller temperatures until it eventually fails when $T \leq |\mu_B^{\text{YL}}(T)|/(3\pi)$.

We see that the program of [18] of using the resummation technique to locate Lee-Yang zeros (or at least the closest zeroes) finds support in our calculation. Note that our calculations are performed in the infinite volume/thermodynamic limit, while lattice QCD calculations are intrinsically finite volume. We remind the reader that, in the mean-field approximation, we are bound to consider the thermodynamic limit. In a finite volume the Yang-Lee edge and the corresponding branch cut will be replaced by set of Lee-Yang zeroes along the direction of cut. The subtle difference between Lee-Yang zeroes and Yang-Lee edge is most probably of no consequence.

V. THERMODYNAMICS

We now turn to thermodynamics of the model. Here we assess the accuracy of how well both the truncated Taylor series and the resummed approach reproduce the results obtained by a direct computation.

In what follows we consider the net baryon density, χ_1 , and the fourth-order cumulant χ_4 defined in Eq. (15). We choose these two quantities for the following reason. Although the baryon density is not very sensitive to the details of the equation of state, it is a key element in defining the equation of state of QCD and is required for the analysis of heavy-ion collision experiments. The fourth order cumulant is a more sensitive probe of the equation of state and is of significance for the experimental search of the critical end point.

We consider two temperatures: one just a little bit above the pseudocritical temperature (see Tab. I) and one below; $T = 170$ and 120 MeV. In Figs. 2 and 3 we show the dependence of the baryon density on real and imaginary chemical potential for these temperatures, respectively. The left panels of these figures show the comparison between the direct calculations of χ_1 with the results obtained by using the truncated Taylor series. From both figures, it is evident that the Yang-Lee edge singularity, whose location $|\mu_B^{\text{YL}}|$ is indicated by the vertical dashed gray lines, limits the radius of the convergence of the series. Increasing the order of the truncation does not improve the convergence of the series for $|\mu_B| \gtrsim |\mu_B^{\text{YL}}|$, as expected. This is true for both $T = 170$ MeV (Fig. 2, left) and $T = 120$ MeV (Fig. 3, left). The differences between both temperatures regarding the convergence behavior are only due to the different radii of convergence from the different locations of the edge singularity, cf. Fig. 1.

The right panels of Figs. 2 and 3 show the comparison between the full result for χ_1 and the resummation for different orders in the expansion of the fermion determinant. As compared to the Taylor expansion in the left panels of the respective figures, the resummation shows superior results without any apparent sensitivity to the radius of convergence defined by the Yang-Lee edge singularity.

The resummation converges rapidly with increasing order of the truncation within the whole region of real and imaginary chemical potentials studied here. χ_1 is accurately described for all orders $N \geq 6$. The convergence at large imaginary chemical potential is slower than at large real chemical potential. This is because the chiral condensate $\bar{\sigma}$ monotonously increases from its value at $\mu_B = 0$ for increasing imaginary chemical potential with $i\mu_B \leq 3i\pi T$, while it monotonously decreases with increasing real chemical potential. In the former case, the simple expansion that leads to Eq. (30) is not possible and the thermodynamic potential is in general a complicated function of μ_B . In the latter case, for large real μ_B , the condensate is very small and Eq. (30) is well approximated by only the first term. It then follows from the properties of the polylogarithm that the thermodynamic potential in Eq. (25) is a fourth-order polynomial in μ_B

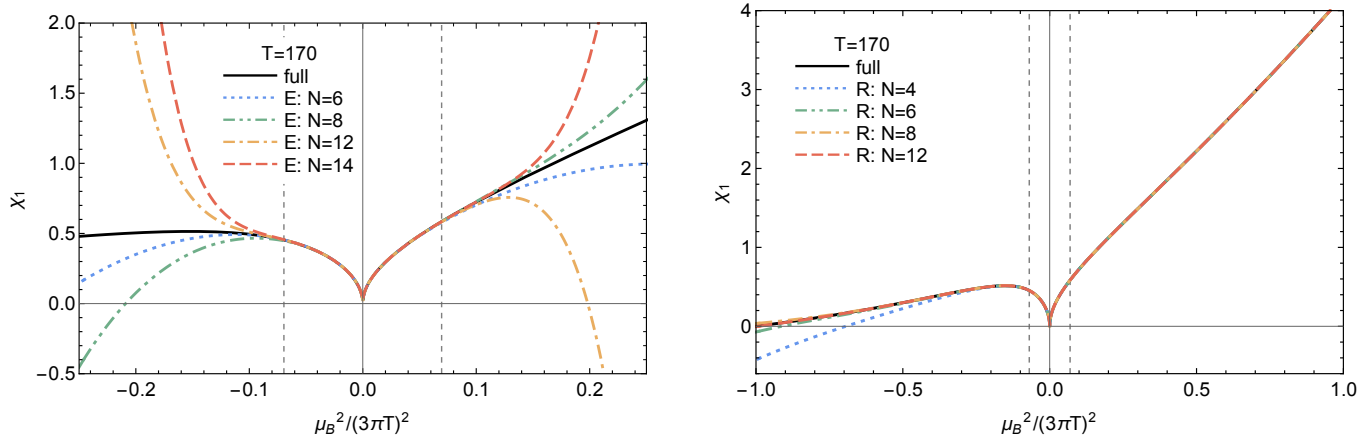


FIG. 2. $\chi_1(\mu_B^2)$ at $T = 170$ MeV for purely real and purely imaginary μ_B . In the latter case, also χ_1 is purely imaginary. The vertical dashed lines denote the location of the edge singularity $|\mu_B^{YL}|$. *Left*: Comparison between the full result and various orders of the Taylor expansion around $\mu = 0$ (E). *Right*: Comparison between the full result and various orders of the resummation (R).

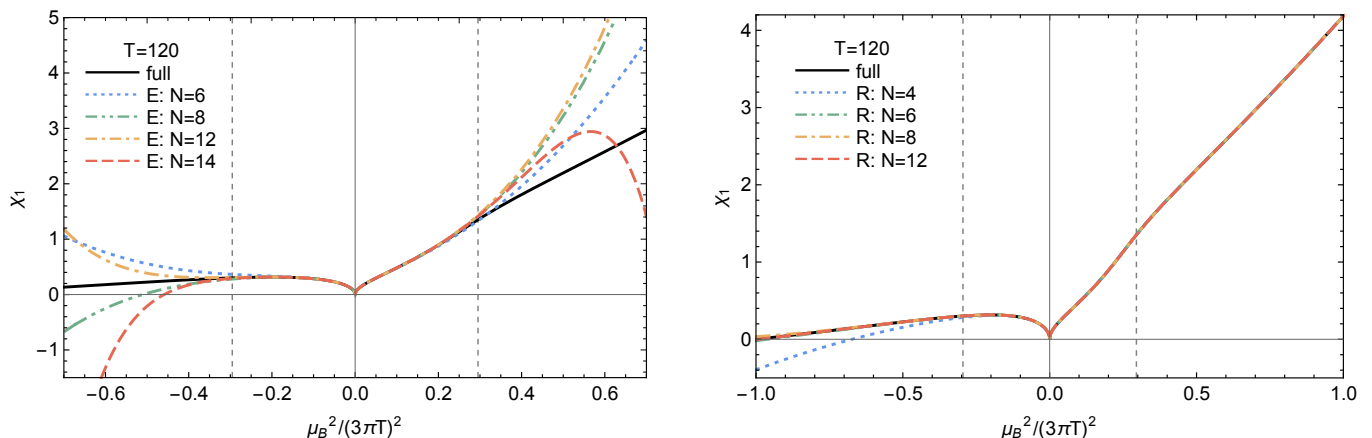


FIG. 3. Same as Fig. 2 with $T = 120$ MeV.

for $|\mu_B| < 3\pi T$ [35]. Thus, for large real μ_B , $\bar{\sigma} \rightarrow 0$ and the potential is that of a free gas of fermions. The resummation at order $N = 4$ already captures this exactly. The Taylor expansion around $\mu_B = 0$ is clearly not able to reproduce this simple asymptotic behavior at any order.

The dependence of the fourth order susceptibility on real and imaginary chemical potentials, $\chi_4(\mu_B)$, is demonstrated in Figs. 4 and 5, again at $T = 170$ and 120 MeV. Since higher order susceptibilities are more sensitive to quark/baryon number fluctuations, χ_4 is in general a more complicated function than χ_1 . It is therefore a stricter test for convergence. Furthermore, rapidly varying/increasing χ_n can be an indication for a crossover transition. This is seen in Fig. 4, where signs of a crossover at imaginary μ_B are shown, and similarly in Fig. 5, where a crossover is indicated at real μ_B . This is expected because the former is at temperatures above T_c , while the latter is below. As can be seen in the left panels of these figures, the Taylor expansion is only converged for a very narrow region around $\mu_B = 0$ for $N \leq 14$. Thus, the order of

the expansion is not high enough to probe the radius of convergence.

The convergence properties of the resummation discussed above for χ_1 , while qualitatively the same, are more apparent in χ_4 . This is shown in the right panels of Figs. 4 and 5. Again, we observe very rapid convergence at real chemical potential. It follows from the previous discussion that χ_4 has to become constant at large real μ_B when the condensate vanishes. This asymptotic behavior, as well as the nontrivial functional form of χ_4 at smaller μ_B , is reproduced with high precision already at low orders of the resummation. The convergence is markedly slower at large imaginary μ_B , but still discernible. The range of validity of the resummation, $|\mu_B| < 3\pi T$, discussed in Sec. IV, is evident here.

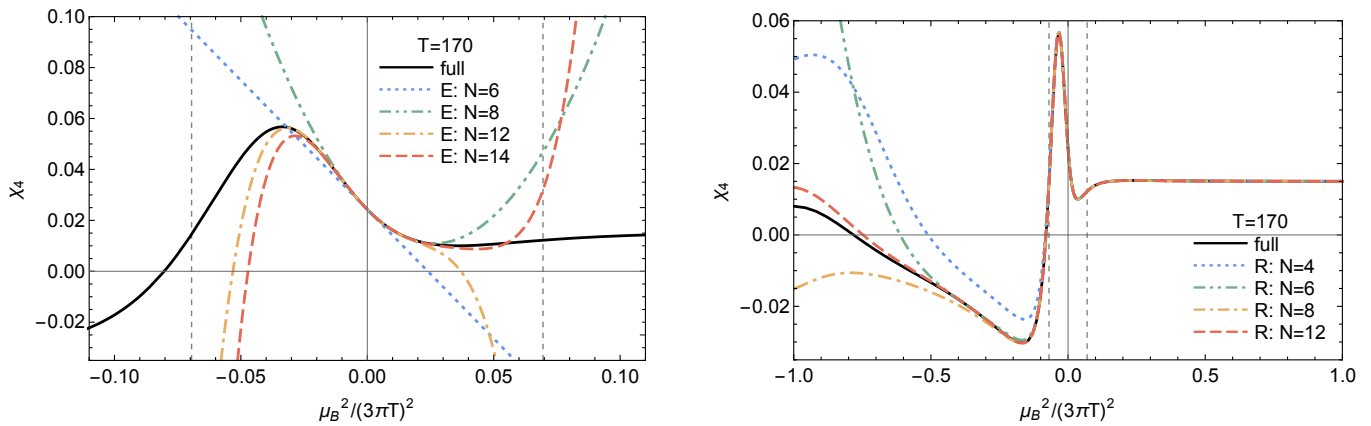


FIG. 4. $\chi_4(\mu_B^2)$ at $T = 170$ MeV for purely real and purely imaginary μ_B . The vertical dashed lines denote the location of the edge singularity $|\mu_B^{YL}|$. *Left*: Comparison between the full result and various orders of the Taylor expansion around $\mu = 0$ (E). *Right*: Comparison between the full result and various orders of the resummation (R).

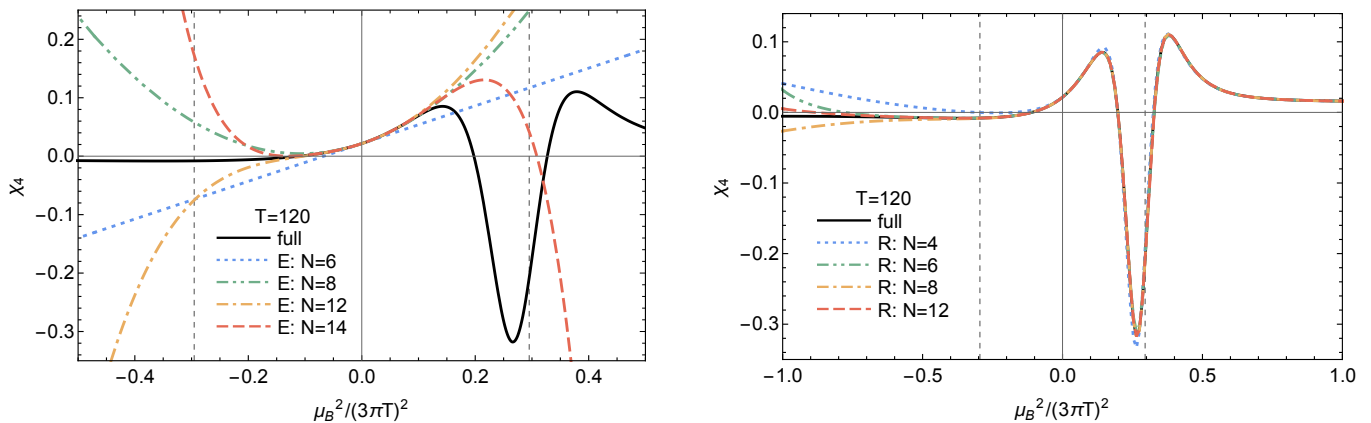


FIG. 5. Same as Fig. 4 with $T = 120$ MeV.

VI. CONCLUSIONS

We have tested the scheme put forward in [18] for the resummation of infinite orders of an expansion of the partition function in the chemical potential in a mean-field quark-meson model. In this case, the resummation amounts to solving the equation of motion based on a series expansion of the effective potential. As a result, the bosonic mean-field becomes a nontrivial function of the chemical potential. This directly translates into a mean-field thermodynamic potential with nontrivial, in general nonanalytic, dependence on the chemical potential. This way, not only the effects of infinite powers in the chemical potential are taken into account, but also the analytic structure of the partition function becomes accessible.

This is in contrast to an ordinary Taylor expansion of the thermodynamic potential in powers of the chemical potential, as it is by definition strictly analytic and therefore bound to fail whenever nonanalyticities determine the structure of the partition function. The relevant singularities here are thermal cuts arising from thermal distributions in the partition function, and the Yang-Lee

edge singularity, which is a critical point and a branch point singularity in the complex chemical potential plane.

By confronting the results of a direct computation at finite density with the resummation method and the Taylor expansion, we have tested the capabilities of describing the analytical structure and the thermodynamics of the model at finite density. We have found that the resummation is far superior in describing the model at finite chemical potential as compared to the Taylor expansion. In fact, the resummation at truncation order $N = 8$ already describes the susceptibilities for all real and imaginary chemical potentials studied here with high accuracy. Furthermore, the location of the Yang-Lee edge singularity is also described accurately for $T \gtrsim 90$ MeV.

Since the resummation is able to capture important analytical features of the equation of state at finite chemical potential, it is not limited by the same analytical constraints as the Taylor expansion. As expected, the Taylor expansion breaks down at the location of the edge singularity, since it defines its radius of convergence. Even high orders of the Taylor expansion fail to describe the nontrivial μ_B -dependence of higher-order susceptibilities already

at small μ_B . In contrast, since infinite orders in μ_B are taken into account with the resummation, the nontrivial functional form of higher order susceptibilities, as well as their asymptotic behavior at large $\mu_B > 0$, is reproduced faithfully. We find that the resummation with increasing order of the truncation converges rapidly for chemical potentials in the region $-(3\pi T)^2 \leq \mu_B^2 \lesssim (3\pi T)^2$. The only strict limit on the applicability of the resummation stems from the fact that the thermal cuts cannot be captured, limiting its range of validity to $|\mu_B| < 3\pi T$ in the quark-meson model. In the confined phase of QCD this bound would be decreased to $|\mu_B| < \pi T$, as thermal distributions of baryons, rather than quarks, determine the thermal cuts in QCD.

We point out that the resummation is not aimed at curing or mitigating the sign problem; as for any reweighting method, Eq. (5) has a sign problem. The goal is to capture the singularities in the complex plane in order to extend lattice computations to these values of μ_B . The purpose of the present work has been to test whether or not the analytical structure can be captured by the

resummation.

To further test the resummation scheme, a study analogous to the present one, but beyond mean-field, would be useful. In any case, the present work demonstrates the capability of this scheme in resolving the analytical structure and thermodynamics of a nontrivial theory for a wide range of complex chemical potentials. Our results therefore provide strong indications for the advantages of using the resummation scheme also for theories like QCD at finite baryochemical potential, as studied in [18].

ACKNOWLEDGEMENT

We thank G. Johnson and R. Pisarski for stimulating discussions. This material is based upon work supported by the U.S. Department of Energy, Office of Science, Office of Nuclear Physics through the Contract Nos. DE-SC0012704 (SM, FR), DE-SC0020081 (VS) and the Beam Energy Scan Theory (BEST) Topical Collaboration.

-
- [1] X. An *et al.*, The BEST framework for the search for the QCD critical point and the chiral magnetic effect, (2021), [arXiv:2108.13867 \[nucl-th\]](#).
- [2] G. Aarts, Can complex Langevin dynamics evade the sign problem?, *PoS LAT2009*, 024 (2009), [arXiv:0910.3772 \[hep-lat\]](#).
- [3] G. Aarts, L. Bongiovanni, E. Seiler, D. Sexty, and I.-O. Stamatescu, Controlling complex Langevin dynamics at finite density, *Eur. Phys. J. A* **49**, 89 (2013), [arXiv:1303.6425 \[hep-lat\]](#).
- [4] D. Sexty, Simulating full QCD at nonzero density using the complex Langevin equation, *Phys. Lett. B* **729**, 108 (2014), [arXiv:1307.7748 \[hep-lat\]](#).
- [5] Z. Fodor, S. D. Katz, D. Sexty, and C. Török, Complex Langevin dynamics for dynamical QCD at nonzero chemical potential: A comparison with multiparameter reweighting, *Phys. Rev. D* **92**, 094516 (2015), [arXiv:1508.05260 \[hep-lat\]](#).
- [6] M. Cristoforetti, F. Di Renzo, and L. Scorzato (Aurora-Science), New approach to the sign problem in quantum field theories: High density QCD on a Lefschetz thimble, *Phys. Rev. D* **86**, 074506 (2012), [arXiv:1205.3996 \[hep-lat\]](#).
- [7] M. Fukuma, N. Matsumoto, and N. Umeda, Implementation of the HMC algorithm on the tempered Lefschetz thimble method, (2019), [arXiv:1912.13303 \[hep-lat\]](#).
- [8] A. Alexandru, G. Basar, P. F. Bedaque, and N. C. Warrington, Complex Paths Around The Sign Problem, (2020), [arXiv:2007.05436 \[hep-lat\]](#).
- [9] C. S. Fischer, QCD at finite temperature and chemical potential from Dyson–Schwinger equations, *Prog. Part. Nucl. Phys.* **105**, 1 (2019), [arXiv:1810.12938 \[hep-ph\]](#).
- [10] W.-j. Fu, J. M. Pawłowski, and F. Rennecke, QCD phase structure at finite temperature and density, *Phys. Rev. D* **101**, 054032 (2020), [arXiv:1909.02991 \[hep-ph\]](#).
- [11] A. Bazavov *et al.*, The QCD Equation of State to $\mathcal{O}(\mu_B^6)$ from Lattice QCD, *Phys. Rev. D* **95**, 054504 (2017), [arXiv:1701.04325 \[hep-lat\]](#).
- [12] S. Datta, R. V. Gavai, and S. Gupta, Quark number susceptibilities and equation of state at finite chemical potential in staggered QCD with $N_t=8$, *Phys. Rev. D* **95**, 054512 (2017), [arXiv:1612.06673 \[hep-lat\]](#).
- [13] S. Borsányi, Z. Fodor, J. N. Guenther, R. Kara, S. D. Katz, P. Parotto, A. Pásztor, C. Ratti, and K. K. Szabó, Lattice QCD equation of state at finite chemical potential from an alternative expansion scheme, *Phys. Rev. Lett.* **126**, 232001 (2021), [arXiv:2102.06660 \[hep-lat\]](#).
- [14] R. V. Gavai and S. Gupta, QCD at finite chemical potential with six time slices, *Phys. Rev. D* **78**, 114503 (2008), [arXiv:0806.2233 \[hep-lat\]](#).
- [15] F. Karsch, B.-J. Schaefer, M. Wagner, and J. Wambach, Towards finite density QCD with Taylor expansions, *Phys. Lett. B* **698**, 256 (2011), [arXiv:1009.5211 \[hep-ph\]](#).
- [16] G. Basar, Universality, Lee-Yang Singularities, and Series Expansions, *Phys. Rev. Lett.* **127**, 171603 (2021), [arXiv:2105.08080 \[hep-th\]](#).
- [17] C. Schmidt, J. Goswami, G. Nicotra, F. Ziesché, P. Dimopoulos, F. Di Renzo, S. Singh, and K. Zambello, Net-baryon number fluctuations, in *Criticality in QCD and the Hadron Resonance Gas* (2021) [arXiv:2101.02254 \[hep-lat\]](#).
- [18] S. Mondal, S. Mukherjee, and P. Hegde, Lattice QCD Equation of State for Nonvanishing Chemical Potential by Resumming Taylor Expansions, *Phys. Rev. Lett.* **128**, 022001 (2022), [arXiv:2106.03165 \[hep-lat\]](#).
- [19] D. U. Jungnickel and C. Wetterich, Effective action for the chiral quark-meson model, *Phys. Rev. D* **53**, 5142 (1996), [arXiv:hep-ph/9505267](#).
- [20] B.-J. Schaefer and J. Wambach, The Phase diagram of the quark meson model, *Nucl. Phys. A* **757**, 479 (2005), [arXiv:nucl-th/0403039](#).
- [21] V. Skokov, B. Friman, E. Nakano, K. Redlich, and B. J. Schaefer, Vacuum fluctuations and the thermodynamics of chiral models, *Phys. Rev. D* **82**, 034029 (2010), [arXiv:1005.3166 \[hep-ph\]](#).

- [22] J. M. Pawłowski and F. Rennecke, Higher order quark-mesonic scattering processes and the phase structure of QCD, *Phys. Rev. D* **90**, 076002 (2014), [arXiv:1403.1179 \[hep-ph\]](#).
- [23] S. Resch, F. Rennecke, and B.-J. Schaefer, Mass sensitivity of the three-flavor chiral phase transition, *Phys. Rev. D* **99**, 076005 (2019), [arXiv:1712.07961 \[hep-ph\]](#).
- [24] C. R. Allton, M. Doring, S. Ejiri, S. J. Hands, O. Kaczmarek, F. Karsch, E. Laermann, and K. Redlich, Thermodynamics of two flavor QCD to sixth order in quark chemical potential, *Phys. Rev. D* **71**, 054508 (2005), [arXiv:hep-lat/0501030](#).
- [25] M. Giordano, K. Kapas, S. D. Katz, D. Negradi, and A. Pasztor, New approach to lattice QCD at finite density; results for the critical end point on coarse lattices, *JHEP* **05**, 088, [arXiv:2004.10800 \[hep-lat\]](#).
- [26] S. Borsanyi, Z. Fodor, M. Giordano, S. D. Katz, D. Negradi, A. Pasztor, and C. H. Wong, Lattice simulations of the QCD chiral transition at real baryon density, *Phys. Rev. D* **105**, L051506 (2022), [arXiv:2108.09213 \[hep-lat\]](#).
- [27] C.-N. Yang and T. D. Lee, Statistical theory of equations of state and phase transitions. 1. Theory of condensation, *Phys. Rev.* **87**, 404 (1952).
- [28] T. D. Lee and C.-N. Yang, Statistical theory of equations of state and phase transitions. 2. Lattice gas and Ising model, *Phys. Rev.* **87**, 410 (1952).
- [29] M. Laine and A. Vuorinen, *Basics of Thermal Field Theory*, Vol. 925 (Springer, 2016) [arXiv:1701.01554 \[hep-ph\]](#).
- [30] M. E. Fisher, Yang-Lee Edge Singularity and ϕ^3 Field Theory, *Phys. Rev. Lett.* **40**, 1610 (1978).
- [31] M. A. Stephanov, QCD critical point and complex chemical potential singularities, *Phys. Rev. D* **73**, 094508 (2006), [arXiv:hep-lat/0603014](#).
- [32] G. A. Almási, B. Friman, K. Morita, and K. Redlich, Fourier coefficients of the net baryon number density and their scaling properties near a phase transition, *Phys. Lett. B* **793**, 19 (2019), [arXiv:1902.05457 \[hep-ph\]](#).
- [33] S. Mukherjee and V. Skokov, Universality driven analytic structure of the QCD crossover: radius of convergence in the baryon chemical potential, *Phys. Rev. D* **103**, L071501 (2021), [arXiv:1909.04639 \[hep-ph\]](#).
- [34] A. Connelly, G. Johnson, F. Rennecke, and V. Skokov, Universal Location of the Yang-Lee Edge Singularity in $O(N)$ Theories, *Phys. Rev. Lett.* **125**, 191602 (2020), [arXiv:2006.12541 \[cond-mat.stat-mech\]](#).
- [35] D. Wood, *The Computation of Polylogarithms*, Tech. Rep. 15-92* (University of Kent, Computing Laboratory, University of Kent, Canterbury, UK, 1992).